First Clinical Results of (D)-^{18}F-Fluoromethyltyrosine (BAY 86-9596) PET/CT in Patients with Non–Small Cell Lung Cancer and Head and Neck Squamous Cell Carcinoma

Irene A. Burger[1], Sabine Zitzmann-Kolbe[2], Jan Pruim[3], Matthias Friebe[4], Keith Graham[2], Andrew Stephens[4], Ludger Dinkelborg[4], Kristin Kowal[2], Roger Schibli[5], Gert Luurtsema[3], Bram Maas[3], Michaela Horn-Tutic[6], Stephan K. Haerle[7], Johan Wiegers[3], Niklaus G. Schaefer[1,8], Thomas F. Hany[9], and Gustav K. von Schulthess[1]

[1]Division of Nuclear Medicine, Department of Medical Radiology, University Hospital of Zurich, Zurich, Switzerland; [2]Bayer Healthcare AG, Berlin, Germany; [3]Department of Nuclear Medicine and Molecular Imaging, University Medical Center Groningen, Groningen, The Netherlands; [4]Piramal Imaging GmbH, Berlin, Germany; [5]Center for Radiopharmaceutical Sciences of ETH, PSI, and USZ, ETH Zurich, Zurich, Switzerland; [6]Department of Thoracic Surgery, University Hospital of Zurich, Zurich, Switzerland; [7]Department of Otolaryngology–Head and Neck Surgery, University Hospital of Bale, Bale, Switzerland; [8]Division of Medical Oncology, Department of Internal Medicine, University Hospital of Zurich, Zurich, Switzerland; and [9]MRI Stadelhofen, Zurich, Switzerland

(D)-^{18}F-fluoromethyltyrosine (D-^{18}F-FMT), or BAY 86-9596, is a novel ^{18}F-labeled tyrosine derivative rapidly transported by the L-amino acid transporter (LAT-1), with a faster blood pool clearance than the corresponding L-isomer. The aim of this study was to demonstrate the feasibility of tumor detection in patients with non–small cell lung cancer (NSCLC) or head and neck squamous cell cancer (HNSCC) compared with inflammatory and physiologic tissues in direct comparison to ^{18}F-FDG. **Methods:** 18 patients with biopsy-proven NSCLC (n = 10) or HNSCC (n = 8) were included in this Institutional Review Board–approved, prospective multicenter study. All patients underwent ^{18}F-FDG PET/CT scans within 21 d before D-^{18}F-FMT PET/CT. For all patients, safety and outcome data were assessed. **Results:** No adverse reactions were observed related to D-^{18}F-FMT. Fifty-two lesions were ^{18}F-FDG–positive, and 42 of those were malignant (34 histologically proven and 8 with clinical reference). Thirty-two of the 42 malignant lesions were also D-^{18}F-FMT–positive, and 10 lesions had no tracer uptake above the level of the blood pool. Overall there were 34 true-positive, 8 true-negative, 10 false-negative, and only 2 false-positive lesions for D-^{18}F-FMT, whereas ^{18}F-FDG was true-positive in 42 lesions, with 10 false-positive and only 2 false-negative, resulting in a lesion-based detection rate for D-^{18}F-FMT and ^{18}F-FDG of 77% and 95%, respectively, with an accuracy of 78% for both tracers. A high D-^{18}F-FMT tumor–to–blood pool ratio had a negative correlation with overall survival (P = 0.050), whereas the ^{18}F-FDG tumor–to–blood pool ratio did not correlate with overall survival. **Conclusion:** D-^{18}F-FMT imaging in patients with NSCLC and HNSCC is safe and feasible. The presented preliminary results suggest a lower sensitivity but higher specificity for D-^{18}F-FMT over ^{18}F-FDG, since there is no D-^{18}F-FMT uptake in inflammation. This increased specificity may be particularly beneficial in areas with endemic granulomatous disease and may improve clinical management. Further clinical investigations are needed to determine its clinical value and relevance for the prediction of survival prognosis.

Key Words: D-amino acid transport system; LAT-1; tumor staging; specificity; FDG

J Nucl Med 2014; 55:1778–1785
DOI: 10.2967/jnumed.114.140699

Despite the widespread use and success of ^{18}F-FDG PET/CT for cancer imaging, the potential benefits of amino acid–based tracers with a potentially higher specificity have been discussed and investigated in the past (*1*). Especially, the well-known accumulation of ^{18}F-FDG in inflammatory lesions—indistinguishable from tumor accumulation—can lead to over-staging of patients. One well-established concept for improved tumor specificity is the increased expression of amino acid transporters in transformed cancer cells, leading to increased accumulation of amino acids in tumor cells (*2*). The general feasibility of amino acid imaging in different tumor types has been demonstrated extensively (*3*). However, several studies have shown an insufficient sensitivity for some amino acid tracers, for example, *O*-2-^{18}F-fluoroethyl-L-tyrosine (^{18}F-FET) for head and neck cancer (*4–6*). The situation is different for brain tumors, for which ^{18}F-FET is established and helpful in differentiating inflammatory from cancerous lesions and in tumor grading (*7*). Furthermore, ^{18}F-FET has added value in therapy assessment after surgery or radiotherapy of malignant gliomas (*8*).

(D)-^{18}F-fluoromethyltyrosine (D-^{18}F-FMT), or BAY 86-9596, is a new diagnostic amino acid PET tracer. Close bioisosteres of L-amino acids labeled for imaging with ^{18}F tend to behave like their naturally occurring counterparts, and some are integrated and metabolized by mammalian cells, resulting in a significant uptake in nontumorous cells, whereas D-isomers are characterized by a faster clearance (*9*). The principle of using D-amino tyrosine derivatives was introduced by Tsukada et al. (*10,11*). Comparison of D-^{18}F-FMT with other "alkyl"-tyrosines showed the superiority of D-^{18}F-FMT over D- and L-^{18}F-FET or D- and L-fluoropropyltyrosine regarding tumor uptake rate in mice (*10*). These results suggest that tumor uptake decreases with an increasing length of the alkyl chain carrying the ^{18}F label. A high tumor accumulation of D-^{18}F-FMT along with a rapid blood pool clearance resulted in favorable

Received Jun. 7, 2014; revision accepted Aug. 14, 2014.
For correspondence or reprints contact: Irene A. Burger, Nuclear Medicine, University Hospital Zurich, Ramistrasse 100, CH-8091 Zurich, Switzerland.
E-mail: irene.burger@usz.ch
Published online Sep. 25, 2014.

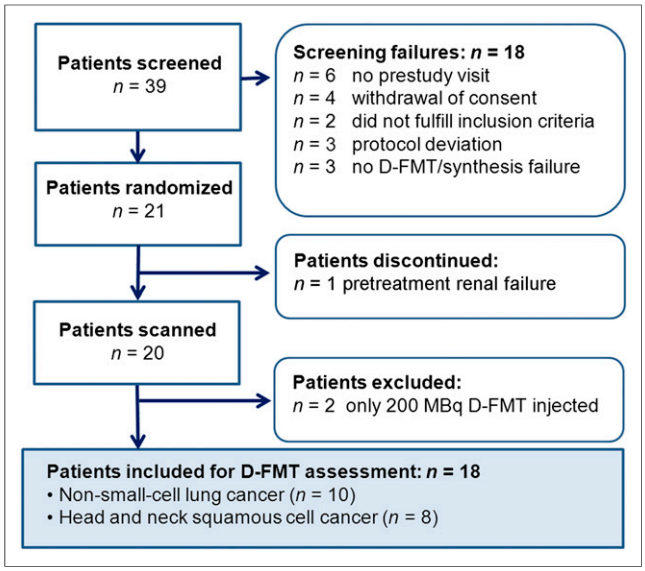

FIGURE 1. Patient selection.

images with significant tumor–to–blood pool and tumor-to-organ ratios for D-^{18}F-FMT in tumor-bearing mice and rats (*12*) and could also be confirmed in a mouse bone metastasis model originating from renal cancer cells (*13*). D-^{18}F-FMT was successful in monitoring the radiotherapy response of tumors in mice bearing tumors with a squamous cell carcinoma cell line (*14*).

A significant limitation of ^{18}F-FDG PET imaging is the accumulation in inflamed tissues, leading to false-positive results (*15*). D-^{18}F-FMT proved to have no accumulation in turpentine-induced inflammatory tissue in a mouse model, whereas ^{18}F-FDG displayed significant uptake and retention (*11*).

Therefore D-^{18}F-FMT could supersede the currently used tyrosine derivatives because of its significant tumor uptake and rapid clearance, potentially resulting in an earlier image acquisition and improved tumor-to-background levels. Herein, the first results, to our knowledge, are reported on the tracer safety and diagnostic potential of D-^{18}F-FMT in patients with head and neck squamous cell cancer (HNSCC) and patients with non–small cell lung cancer (NSCLC).

MATERIALS AND METHODS

Patients

This prospective study was performed in 2 centers and approved by the Institutional Review Board of each. The conduct of the study met all local legal and regulatory requirements and was in accordance with the ethical principles originating from International Conference on Harmonization guideline E6: Good Clinical Practice. To be included in the study, patients had to give written informed consent; be between 30 and 80 y old; if female, either have no childbearing potential or not be pregnant or nursing; have an Eastern Cooperative Oncology Group performance status of 0–2; have a life expectancy of more than 3 mo; and have confirmation of adequate function of major organ systems. In addition, inclusion in the study required that patients have undergone clinically indicated ^{18}F-FDG PET/CT for staging, restaging, or therapy response assessment that showed a tumor mass with ^{18}F-FDG uptake and a high certainty for NSCLC or HNSCC, followed within 21 d by D-^{18}F-FMT PET/CT, with no chemotherapy, radiotherapy, or immune/biologic therapy or biopsy performed or scheduled between the 2 scans. The final inclusion criterion was histopathologic or cytologic confirmation of malignancy.

Safety data were acquired for each patient 1 d before the scan, after the scan, and 1 d after D-^{18}F-FMT PET/CT injection. Clinical follow-up data were collected for all patients.

Image Acquisition and Analysis

^{18}F-FDG PET/CT Scan. All patients were first examined using a routine clinical protocol on an integrated PET/CT scanner (GE Healthcare DSTX, 64-slice CT [GE Health Systems], or Biograph mCT 4-64 PET/CT [Siemens]) with injection of 350 MBq of ^{18}F-FDG 60 min before the examination. PET/CT was acquired from the mid thigh to the vertex of the skull with scan times of 2–3 min per frame. Every patient fasted for at least 4 h, and blood glucose levels were not elevated (<8 mmol/L). A low-dose unenhanced CT scan was obtained (80 mAs, 140 kVp, 0.5 s/tube rotation, pitch of 1.7, and slice thickness of 3.75 mm) (*16*).

TABLE 1
Clinical Data for NSCLC

Patient no.	Sex	Age (y)	Body weight (kg)	Lesion type	Location of primary tumor	^{18}F-FDG PET indication	Staging	^{18}F-FMT dose (MBq)	Specific activity* (GBq/μmol)
1	M	59	83	AC	Right upper lobe	Staging	T1 N2 M0	302	19.4
2	F	51	109	AC	Left upper lobe	Staging	T1 N2 M0	320	19.3
3	F	60	48	SCC	Middle lobe	Staging	T4 N0 pM1	288	15.8
4	M	68	115	AC	Right lower lobe	Staging	T2b N2 M0	312	14.8
5	F	69	40	SCC	Left lower lobe	Staging	T4 N2 M0	294	31.6
6	F	77	55	AC	Left lower lobe	Staging	T3 N2 M1a	300	24.8
7	F	64	41	SCC	Left lower lobe	Restaging	T3 N0 M0	294	32.1
8	M	52	84	SCC	Left upper lobe	Staging	T2 N2 M0	325	102
9	M	59	75	AC	Right upper lobe	Staging	T2 N2 M0	303	180
10	M	65	93	AC	Right lower lobe	Restaging	T3 N3 M1a	307	170

*Specific activity at time point of injection.
AC = adenocarcinoma; SCC = squamous cell carcinoma.

TABLE 2
Clinical Data for HNSCC

Patient no.	Sex	Age (y)	Body weight (kg)	Lesion type	Location of primary tumor	^{18}F-FDG PET indication	Staging	^{18}F-FMT dose (MBq)	Specific activity* (GBq/μmol)
1	M	50	58	SCC	Hypopharyngeal	Staging	T4 N2 M0	306	31.8
2	M	70	75	SCC	Laryngeal	Staging	T3 N2c M0	300	25.5
3	M	67	84	SCC	Oropharynx	Staging	T4 N3 M0	304	82.2
4	M	64	77	SCC	Tongue	Staging	T2 N2a M0	306	38.5
5	M	68	70	SCC	Oropharynx	Restaging	T3 N2 M0	318	83.9
6	M	48	113	SCC	Oropharynx	Staging	T1 N2b M0	324	57.2
7	M	44	89	SCC	Oropharynx	Staging	T4 N2c M0	303	47.4
8	M	67	83	SCC	Hypopharyngeal	Restaging	T2 N2 M0	316	38.2

*Specific activity at time point of injection.
SCC = squamous cell carcinoma.

D-^{18}F-FMT PET/CT Scan. All patients were injected with 300 MBq of D-^{18}F-FMT. For the first 6 patients, a 20-min dynamic PET acquisition was started at the tumor region right after injection. Afterward, 3 whole-body PET images were acquired after 30, 45, and 60 min. These data were used to determine the optimal imaging time point for D-^{18}F-FMT. In an interim assessment before patient 7, it was decided to obtain 2 whole-body D-^{18}F-FMT scans, the first at 30 min after injection and the second at 45 min, for patients 7–20.

Image Analysis

^{18}F-FDG images were analyzed by 2 dual-board-certified nuclear medicine physicians and radiologists in consensus. D-^{18}F-FMT images were analyzed by the same readers, with a direct comparison of both scans.

Lesions suggestive of or unequivocal for malignant involvement were visually judged for ^{18}F-FDG and D-^{18}F-FMT activity, with − indicating no increased uptake, + indicating just slightly increased uptake (more than background), and ++ indicating markedly increased uptake.

Furthermore, a quantitative analysis of ^{18}F-FDG versus D-^{18}F-FMT accumulation was performed using the maximum standardized uptake value (SUV_{max}) ratios of tumor to blood pool to determine the relative uptake into malignant tissue.

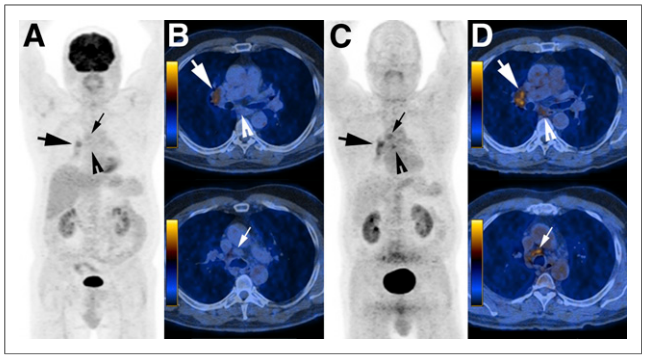

FIGURE 2. Non–small cell lung cancer in right hilum with mediastinal lymph node metastases. (A and B) ^{18}F-FDG PET with mild active primary tumor (large arrow) and ^{18}F-FDG–negative lymph node metastases (arrowhead and small arrow). (C and D) D-^{18}F-FMT PET with higher uptake in primary tumor (large arrow) and positive uptake in ipsilateral and infracarinal mediastinal lymph node metastases (arrowhead and small arrow). A and C are coronal views; B and D are axial views.

D-^{18}F-FMT Preparation

The radionuclide ^{18}F and the drug substance (*R*)-2-amino-3-(4-^{18}F-fluoromethoxyphenyl)-propionic acid hydrochloride were produced at both clinical sites, starting from a precursor compound that had been produced following good manufacturing practice guidelines. D-^{18}F-FMT was synthesized as previously described (*11*).

Statistical Analysis

Quantitative data are expressed as mean ± SD if normally distributed or as median with ranges if nonnormally distributed. Diagnostic performance, detection rate, and accuracy were determined by comparing the results of D-^{18}F-FMT PET/CT and ^{18}F-FDG PET/CT with the standard of reference on a per-patient and per-lesion base using the χ^2 test for related variables. Patients were divided into groups above and below the median of the tumor-to-background ratio for D-^{18}F-FMT and ^{18}F-FDG, and Kaplan–Meier graphs were generated to determine associations between tracer uptake and overall survival for NSCLC and HNSCC (significance was determined using the log rank [Mantel-Cox] test).

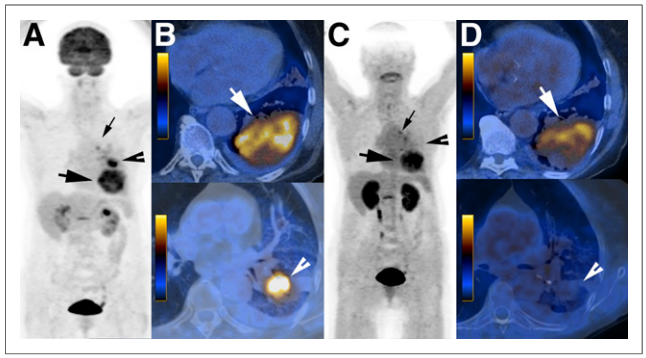

FIGURE 3. Non–small cell lung cancer in left lower lobe with ipsilateral mediastinal lymph node metastasis. (A and B) ^{18}F-FDG PET/CT with primary tumor (large arrow) and 1 mediastinal lymph node metastasis in level 5 (small arrow). (B) Round ^{18}F-FDG–avid consolidation in left superior segment with high ^{18}F-FDG-activity interpreted as metastasis or secondary carcinoma (arrowhead). (C and D) D-^{18}F-FMT PET with uptake in primary tumor (large arrow) and mediastinal lymph node metastasis (small arrow). (D) Consolidation in superior-lower-lobe segment is not D-^{18}F-FMT–avid; on CT follow-up scan this lesion resolved within 2 wk after antibiotic therapy, consistent with pneumonia. A and C are coronal views; B and D are axial views.

TABLE 3
NSCLC: 10 Patients

Patient no.	Lesion type	^{18}F-FDG initial result	^{18}F-FDG T/BP	^{18}F-FMT initial result	^{18}F-FMT T/BP	Lesion size (cm)	Confirmation	^{18}F-FDG final result	^{18}F-FMT final result	^{18}F-FDG accuracy	^{18}F-FMT accuracy
1	Primary tumor (AC)	+	1.5	++	2.1	2	Histopathology	TP	TP	Understaged: N1	Correct
	Lymph node, hilar ipsilateral	+	1.1	+	1.7	0.8	Histopathology	TP	TP		
	Lymph node, mediastinal ipsilateral	−	−	+	1.6	1.2	Histopathology	FN	TP		
	Lymph node, mediastinal ipsilateral	−	−	+	1.5	1.2	Histopathology	FN	TP		
2	Primary tumor (AC)	+	1.7	−	0.6	1.5	Histopathology	TP	FN	Overstaged: (M1)	Understaged: (N0)
	Lymph node, hilar ipsilateral	+	2.1	−	−	1	Histopathology	TP	FN		
	Lymph node, mediastinal ipsilateral	+	1.7	−	−	0.8	Histopathology	TP	FN		
	Bone lesion (lumbar spine)	+	1.3	−	−	1.2	MR imaging, spine	FP	TN		
3	Primary tumor (SCC)	++	5.9	+	1.6	4.5	Histopathology	TP	TP	Correct	Correct
4	Primary tumor (AC)	++	6.4	+	1.4	5.7	Histopathology	TP	TP	Correct	Correct
5	Primary tumor (SCC)	++	7.3	++	3.2	6	Histopathology	TP	TP	Overstaged: N3	Correct
	Lymph node, mediastinal ipsilateral	++	3.1	+	1.5	1.7	Histopathology	TP	TP		
	Lymph node, hilar contralateral	+	1.4	−	−	0.9	Histopathology	FP	TN		
6	Primary tumor (AC)	++	3.2	++	2.1	6.8	Histopathology	TP	TP	Overstaged M1b	Overstaged M1b
	Lymph node, hilar ipsilateral	+	1.7	+	1.3	1.2	CT follow-up	TP	TP		
	Ipsilateral lung lesion, different lobe	++	3.6	−	−	1.9	CT follow-up	FP	TN		
	Bone lesion (lumbar spine)	+	2	+	0.9	2.5	MR imaging, spine	FP	FP		
7	Primary tumor (SCC)	++	5.7	+	1	4.5	Histopathology	TP	TP	Correct	Correct
8	Primary tumor (SCC)	++	6.5	+	1.3	5	Histopathology	TP	TP	Correct	Correct
	Bone lesion (cervical spine)	+	1.2	+	1.4	1.1	MR imaging, spine	FP	FP		
9	Primary tumor (AC)	+	3	−	−	1.2	Histopathology	TP	FN	Overstaged	Understaged
	Lymph node, hilar ipsilateral	++	7.1	+	1.8	3.5	Histopathology	TP	TP		
	Lung lesion, contralateral	+	2	−	−	5.3	CT follow-up	FP	TN		
10	Primary tumor (AC)	++	6.2	−	−	3.4	Clinical follow-up	TP	FN	Correct	Understaged

T/BP = tumor–to–blood pool ratio; AC = adenocarcinoma; SCC = squamous cell carcinoma; TP = true positive; FN = false negative; FP = false positive; TN = true negative; ++ = markedly increased uptake; + = slightly increased uptake (more than background); − = no increased uptake.

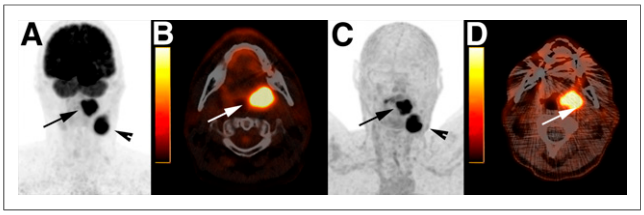

FIGURE 4. Squamous cell carcinoma of left tonsil with 1 large lymph node metastasis (4 cm), left level IIA. (A and B) ^{18}F-FDG PET with active primary tumor (arrow) and clearly positive lymph node metastasis (arrowhead). (C and D) D-^{18}F-FMT PET with high uptake in primary tumor (arrow) and equally high uptake in cervical lymph node metastasis (arrowhead). A and C are coronal views; B and D are axial views.

RESULTS

Patient Characteristic

Thirty-nine patients were screened, of which 18 were not randomized. One patient was excluded after randomization before D-^{18}F-FMT injection because of acute renal failure. Two patients were excluded after the D-^{18}F-FMT scan, because the requested study dose of 300 MBq of D-^{18}F-FMT was not achieved; both patients received only 200 MBq of D-^{18}F-FMT (Fig. 1). The mean delay between the scans was 7 ± 5.1 d (with a range of 1–18 d).

A total of 18 patients (13 men and 5 women), 10 with NSCLC and 8 with HNSCC, were included. They ranged in age from 44 to 77 y (median, 64 y). In total, 54 suggestive lesions were identified; 52 were ^{18}F-FDG–positive, with a median tumor–to–blood pool ratio for SUV_{max} of 3.2 (range, 1.1–7.3). The absolute median uptake for ^{18}F-FDG was an SUV_{max} of 8.9 ± 4.3 (range, 2.2–20.5). Thirty-four malignant lesions were D-^{18}F-FMT–positive, with a median tumor–to–blood pool ratio for SUV_{max} of 1.5 (range, 1–3.2) and absolute values for SUV_{max} of 4.6 ± 1.6 (range, 2.1–8.7). Only 2 lesions were negative on ^{18}F-FDG but detected on D-^{18}F-FMT. In 37 lesions, pathologic findings were available as a standard of reference (27 lesions with histologic results and 10 with cytologic results). For 9 lesions, follow-up imaging was used as a standard of reference (3 with MR imaging of the spine, 5 with CT follow-up examinations, and 1 with an ^{18}F-FDG PET/CT follow-up examination). Four lymph nodes, highly suggestive of metastatic involvement on the initial ^{18}F-FDG PET/CT study, did not undergo further evaluation before radiotherapy (SUV_{max} median, 6.1; range, 5.1–11.5). Three lesions could be identified as inflammatory changes in tonsils on physical examination (Tables 1 and 2).

Safety

The injection of 307 MBq (SD, 10.2 MBq; range, 288–325 MBq) of D-^{18}F-FMT was well tolerated. Safety data did not show any alteration in the sequential pre- and postdosing blood values, electrocardiograms, urine testing, or physical examinations.

Results for NSCLC

On a patient-based analysis, ^{18}F-FDG PET/CT correctly staged 5 of 10 patients (50%) and under-staged 1 patient (10%): histopathology confirmed metastases in ipsilateral mediastinal lymph nodes, which were considered reactive on ^{18}F-FDG PET/CT because they were only mildly enlarged and ^{18}F-FDG–negative (Fig. 2). Four patients were over-staged (40%): in 2 patients increased ^{18}F-FDG uptake in osseous lesions was considered suggestive, but follow-up MR imaging proved degenerative changes; in 1 patient pneumonia could not be differentiated from a secondary tumor (Fig. 3); and in 1 patient an ^{18}F-FDG–active contralateral mediastinal lymph node was considered suggestive of metastasis but was negative on pathologic examination (Table 3).

Six of 10 patients (60%) were correctly staged on the basis of the D-^{18}F-FMT scan. Three patients were under-staged (30%): in those patients the primary tumor did not show any D-^{18}F-FMT accumulation above the background level. Only 1 patient (10%) was over-staged, having a D-^{18}F-FMT–positive lesion in the lumbar spine that was considered unequivocal by both readers.

In 10 patients with NSCLC, a total of 24 lesions were identified. On a lesion-based analysis, ^{18}F-FDG PET/CT correctly identified 16 lesions as true-positive, and 13 lesions were true-positive on D-^{18}F-FMT scans. Six lesions were false-positive with ^{18}F-FDG: 3 were degenerative bone changes, 1 was a reactive lymph node, and 2 were pulmonary infiltrates. Two lesions were false-positive on D-^{18}F-FMT, both corresponding to degenerative bone changes. Two lymph nodes were false-negative on ^{18}F-FDG PET, and 5 lesions were false-negative on D-^{18}F-FMT: in 3 cases the primary tumor showed no D-^{18}F-FMT accumulation above the blood pool level, and in 2 cases lymph nodes were missed on D-^{18}F-FMT PET/CT.

For patients with NSCLC, the overall lesion-based analysis for ^{18}F-FDG/D-^{18}F-FMT showed a detection rate of 89%/72% (χ^2, $P = 0.453$), and the accuracy was 67%/71% (χ^2, $P = 0.751$).

Results for HNSCC

On a patient-based analysis, ^{18}F-FDG PET/CT correctly staged 4 of 8 patients (50%) and over-staged 4 patients (50%). In 3 patients high ^{18}F-FDG uptake in the tonsils was considered suggestive, but clinical examination confirmed only inflammatory changes. These tonsils were all D-^{18}F-FMT–negative. On D-^{18}F-FMT, 5 of 8 patients (63%) were correctly staged. Three patients were under-staged (38%): in 1 patient the primary tumor did not show any D-^{18}F-FMT accumulation above the blood pool level, and in 2 patients contralateral or mediastinal lymph nodes were D-^{18}F-FMT–negative.

A total of 30 suggestive lesions were identified for the 8 patients with HNSCC. On a lesion-based analysis, ^{18}F-FDG PET/CT correctly identified 26 lesions as true-positive; on D-^{18}F-FMT scans, 21 lesions were true-positive (Fig. 4). Four lesions were false-positive for ^{18}F-FDG: they consisted of 3 inflammatory changes in the tonsils and 1 reactive lymph node. Five lesions were false-negative on D-^{18}F-FMT: in 1 case the primary tumor showed no D-^{18}F-FMT accumulation above the blood pool level, and in 4 cases lymph node metastases were missed on D-^{18}F-FMT PET/CT (Table 4).

For patients with HNSCC, the overall lesion-based analysis for ^{18}F-FDG/D-^{18}F-FMT showed a detection rate of 100%/81% (χ^2 rejected because there were no false-negative cases for ^{18}F-FDG) and an accuracy of 83%/81% (χ^2, $P = 0.337$).

Taking all 54 lesions into consideration, a detection rate and accuracy of 95% and 78%, respectively, for ^{18}F-FDG and 77% and 78%, respectively, for D-^{18}F-FMT (χ^2, $P = 0.432/P = 0.600$) were achieved.

PET and Survival

After a mean follow-up of 21.6 mo (range, 4.2–40.7 mo), of the 18 patients 8 were alive with disease and 10 had died of disease. The median tumor–to–blood pool ratio was 3.2 for ^{18}F-FDG and 1.5 for D-^{18}F-FMT. Using this as a cutoff, Kaplan–Meier analysis showed a significant negative association between overall survival

TABLE 4
HNSCC: 8 Patients

Patient no.	Lesion type	^{18}F-FDG initial result	^{18}F-FDG T/BP	^{18}F-FMT initial result	^{18}F-FMT T/BP	Lesion size (cm)	Confirmation	^{18}F-FDG final result	^{18}F-FMT final result	^{18}F-FDG accuracy	^{18}F-FMT accuracy
1	Hypopharyngeal cancer	++	4.5	++	2.6	5	Histopathology	TP	TP	Correct	Correct
	Lymph node, level II R	++	1.5	++	2.1	1.7	Cytology	TP	TP		
	Lymph node, level II L	++	1.7	++	2.1	1.7	Cytology	TP	TP		
	Lymph node, level Vb R	++	4.4	+	1.5	0.8	CT follow-up	TP	TP		
	Lymph node, level Vb L	++	3.6	−	−	0.7	CT follow-up	TP	FN		
2	Hypopharyngeal cancer	++	6.0	++	2.9	4	Histopathology	TP	TP	Correct	Correct
	Lymph node, level III R	++	5.1	+	1.1	2	Cytology	TP	TP		
	Lymph node, level IIa L	++	4.9	+	1.1	1.7	Cytology	TP	TP		
	Lymph node, level III L	++	5.2	+	1.5	1	High radiologic suspicion	TP	TP		
	Lymph node, level IV L	+	2.3	+	1.2	0.9	High radiologic suspicion	TP	TP		
3	Oropharyngeal cancer	++	6.4	++	2.3	3.6	Histopathology	TP	TP	Correct	Correct
	Lymph node, level II L	++	6.25	++	2.7	3.3	Cytology	TP	TP		
4	Cancer of tongue, L	++	3.1	+	1.5	3.4	Histopathology	TP	TP	Overstaged	Correct
	Lymph node, level IIb L	+	1.89	++	1.7	1.4	Cytology	TP	TP		
	Lymph node, level IIb L	+	1.9	+	1.3	1.2	Cytology	TP	TP		
	Tonsillary activity, R	+	2.1	−	−	1.5	Clinical follow-up	FP	TN		
5	Oropharyngeal cancer R	++	2.9	+	1.5	3.2	Histopathology	TP	TP	Correct	Understaged (N)
	Lymph node, mediastinal retrocaval	++	3.3	−	−	1.6	High radiologic suspicion	TP	FN		
	Lymph node, mediastinal anterior	+	2.4	−	−	1.3	High radiologic suspicion	TP	FN		
6	Tonsillary cancer, R	++	3	−	−	4.2	Histopathology	TP	FN	Overstaged	Understaged (T)
	Lymph node, level II/III R	++	6.2	++	1.8	1.3	Histopathology	TP	TP		
	Tonsillary activity, L	++	3.2	−	−	4.1	Clinical follow-up	FP	TN		
7	Tonsillary cancer, L	++	4.5	+	1.4	4.6	Histopathology	TP	TP	Overstaged	Correct
	Tonsillary activity, R	++	2.5	−	−	5.2	Clinical follow-up	FP	TN		
	Lymph node, level IIa/b L	++	4.3	+	1.2	4	Cytology	TP	TP		
	Lymph node, level III L	++	3.2	+	1.1	2.3	Cytology	TP	TP		
	Lymph node, level II R	++	3.5	+	1.2	3.5	Cytology	TP	TP		
8	Recurrent lymph node, level III R	++	5.1	+	1.5	1.4	Histopathology	TP	TP	Overstaged	Understaged
	Lymph node, level IIa R	+	2.8	−	−	3	Histopathology	TP	FN		
	Lymph node, mediastinal	++	3.4	−	−	1.5	PET/CT follow-up	FP	TN		

T/BP = tumor–to–blood pool ratio; TP = true positive; FN = false negative; FP = false positive; TN = true negative; ++ = markedly increased uptake; + = slightly increased uptake (more than background); − = no increased uptake.

and D-^{18}F-FMT ($P < 0.05$) but not between overall survival and ^{18}F-FDG ($P = 0.93$) (Table 5; Fig. 5).

DISCUSSION

This study proved that tumor imaging with D-^{18}F-FMT is safe and feasible for NSCLC and for HNSCC.

The hypothesis that D-^{18}F-FMT would lead to an increased tracer accumulation compared with its L-isomer was further supported clinically in NSCLC patients, with a mean SUV_{max} of 4.5 ± 1.5 for D-^{18}F-FMT compared with 1.8 ± 1.0 for L-^{18}F-FMT in the literature (*17*). SUVs, however, are highly variable and depend on scanner properties, dose application, patient weight, and image reconstructions. Therefore, the value of a direct comparison with published L-^{18}F-FMT data is limited. D-^{18}F-FMT could not reach as high a tumor–to–blood pool level as that achieved with ^{18}F-FDG. D-^{18}F-FMT was able to detect more malignant lesions than ^{18}F-FDG in only 1 patient (5%), whereas relevant lesions were missed in 6 patients (33%). On the other hand, ^{18}F-FDG results were false-positive in 10 lesions overall, whereas D-^{18}F-FMT was false-positive in only 2 osseous lesions. MR imaging showed degenerative changes in both areas, with no evidence of malignancy, suggesting a tendency toward better differentiation between malignant and inflamed tissue. The reason for increased D-^{18}F-FMT uptake in sclerotic bone lesions is unclear.

TABLE 5
Kaplan–Meier Survival for D-^{18}F-FMT and ^{18}F-FDG

Overall survival	Median T/BP cutoff	Mean (mo)	SD	95% CI	Significance (log rank) (Mantel-Cox)
D-^{18}F-FMT	<1.5	31.5	4.7	22.2–40.8	
	≥1.5	20.2	3.6	13.2–27.1	0.050*
^{18}F-FDG	<3.2	24.3	5.8	17.1–32.1	
	≥3.2	24.6	3.8	18.4–31.7	0.930

*Statistical significance.
T/BP = tumor–to–blood pool ratio; CI = confidence interval.

Many of the false-positive findings on ^{18}F-FDG scans were due to inflammatory or infectious changes in tonsils, pulmonary infiltrates, or lymph nodes. Although further investigation (clinical examination or biopsy) could help to elucidate the cause of these false-positive findings, further examinations and more tests would be required for those end-stage patients. Especially in areas with endemic granulomatous disease, high uptake in mediastinal lymph nodes can lead to false-positive findings, thereby over-staging patients with NSCLC. A PET tracer with higher specificity would therefore be especially desirable in these areas. The usefulness of L-^{18}F-FMT in sarcoidosis patients has been suggested by Kaira et al., emphasizing the higher specificity of LAT-1 imaging than of ^{18}F-FDG PET for malignant versus inflammatory disease (*18*).

L-^{18}F-FMT has not yet been used clinically in HNSCC patients. The introduction of L-^{18}F-FET for HNSCC, however, yielded promising results for the primary tumors (*6*). L-^{18}F-FET yielded a mean SUV_{max} of 4.4 ± 2.2 in the primary tumor but only 1.4 ± 0.3 in lymph node metastases. Our results showed a mean D-^{18}F-FMT SUV_{max} of 6.2 ± 1.6 in primary HNSCC tumors. D-^{18}F-FMT was false-negative in only 4 lymph node metastases (size, 1.6 ± 1.4 cm; range, 0.7–3 cm) and positive in 15 lymph node metastases, with a mean SUV_{max} of 4.6 ± 1.4. These results further support the hypothesis of a favorable tumor uptake for D-^{18}F-FMT, compared with L-isomers and extended alkyl chains.

Interestingly, we also observed a tendency for NSCLC, with fewer false-negative cases for squamous cell cancer than for adenocarcinoma; this finding was also observed for L-^{18}F-FMT in a larger cohort of 50 NSCLC patients studied by Kaira et al. (*19*). In a subsequent study, they further investigated L-^{18}F-FMT in 98 patients with NSCLC. In this study group, SUV_{max} for L-^{18}F-FMT was an independent and significant predictor of overall survival, whereas ^{18}F-FDG did not reach significance in a multivariate analysis (*17*). This study could confirm a significant negative correlation between a high tumor–to–blood pool ratio for D-^{18}F-FMT and overall survival (P = 0.05), whereas the tumor–to–blood pool ratio for ^{18}F-FDG did not reach significance (P = 0.93). However, these results have to be viewed with caution and may show only a possible trend in this heterogeneous cohort of only 18 patients, taking into account that univariate analysis using dichotomous cutoffs might further reduce the significance of the results.

Additional studies with larger patient cohorts will help to further substantiate the hypothesis of a direct correlation between tumor–to–blood pool ratio and survival prognosis. The main limitation for studies in patients with multiple metastases and for this study in particular is the limited access to histopathologic samples on a lesion-by-lesion basis to define accurate staging.

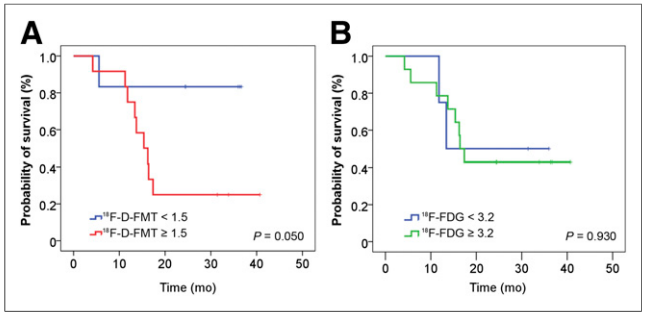

FIGURE 5. Kaplan–Meier curves for overall survival using median tumor–to–blood pool ratio as cutoff for D-^{18}F-FMT (A) and ^{18}F-FDG (B) in 18 patients with NSCLC and HNSCC, illustrating that high D-^{18}F-FMT uptake in both tumor entities might have higher association with adverse outcome than ^{18}F-FDG.

CONCLUSION

This first-in-humans study showed the feasibility and safety of D-^{18}F-FMT imaging in NSCLC and HNSCC. The results showed a trend toward a lower sensitivity for D-^{18}F-FMT than ^{18}F-FDG along with a higher specificity due to the lack of uptake in inflammatory tissues. This finding may lead to improved clinical management of patients in areas with endemic granulomatous disease.

Furthermore, a significant correlation between high D-^{18}F-FMT uptake and overall survival could be shown. Future studies with larger cohorts are needed to show the clinical value of D-^{18}F-FMT for survival prediction and other tumor entities, particularly in comparison to ^{18}F-FDG.

DISCLOSURE

The costs of publication of this article were defrayed in part by the payment of page charges. Therefore, and solely to indicate this fact, this article is hereby marked "advertisement" in accordance with 18 USC section 1734. Matthias Friebe, Andrew Stephens, and Ludger Dinkelborg are affiliated with Piramal Imaging. Kristin Kowal, Sabine Zitzmann-Kolbe, and Keith Graham are employed by Bayer HealthCare. Research support was provided by Bayer Healthcare. No other potential conflict of interest relevant to this article was reported.

ACKNOWLEDGMENTS

We thank the nuclear pharmacy staff, the technologists, and the administrative staff at the University Hospital of Zurich and

University Medical Center Groningen for their help in acquiring the data and freeing up resources. Specifically, we thank Josephine Trinckauf, Verena Weichselbaumer, and Miriam de Bloehme for the data acquisition. Furthermore, we thank Prof. Tsukada of Hamamatsu Photonics for his help and support.

REFERENCES

1. Graf R, Plotkin M, Nyuyki F, et al. Contribution of ^{18}F-fluoro-ethyl-tyrosine positron emission tomography to target volume delineation in stereotactic radiotherapy of malignant cranial base tumours: first clinical experience. *Int J Mol Imaging.* 2012:412585.
2. Christensen HN. Role of amino acid transport and countertransport in nutrition and metabolism. *Physiol Rev.* 1990;70:43–77.
3. Jager PL, Vaalburg W, Pruim J, de Vries EG, Langen KJ, Piers DA. Radiolabeled amino acids: basic aspects and clinical applications in oncology. *J Nucl Med.* 2001;42:432–445.
4. Haerle SK, Fischer DR, Schmid DT, Ahmad N, Huber GF, Buck A. F-18-FET PET/CT in advanced head and neck squamous cell carcinoma: an intra-individual comparison with F-18-FDG PET/CT. *Mol Imaging Biol.* 2011;13:1036–1042.
5. Balogova S, Perie S, Kerrou K, et al. Prospective comparison of FDG and FET PET/CT in patients with head and neck squamous cell carcinoma. *Mol Imaging Biol.* 2008;10:364–373.
6. Pauleit D, Zimmermann A, Stoffels G, et al. ^{18}F-FET PET compared with ^{18}F-FDG PET and CT in patients with head and neck cancer. *J Nucl Med.* 2006;47:256–261.
7. Rapp M, Heinzel A, Galldiks N, et al. Diagnostic performance of ^{18}F-FET PET in newly diagnosed cerebral lesions suggestive of glioma. *J Nucl Med.* 2013;54: 229–235.
8. Niyazi M, Jansen N, Ganswindt U, et al. Re-irradiation in recurrent malignant glioma: prognostic value of [^{18}F]FET-PET. *J Neurooncol.* 2012;110:389–395.
9. Bauwens M, Keyaerts M, Lahoutte T, et al. Intra-individual comparison of the human biodistribution and dosimetry of the D and L isomers of 2-[^{123}I]iodophenylalanine. *Nucl Med Commun.* 2007;28:823–828.
10. Tsukada H, Sato K, Fukumoto D, Kakiuchi T. Evaluation of D-isomers of O-^{18}F-fluoromethyl, O-^{18}F-fluoroethyl and O-^{18}F-fluoropropyl tyrosine as tumour imaging agents in mice. *Eur J Nucl Med Mol Imaging.* 2006;33:1017–1024.
11. Tsukada H, Sato K, Fukumoto D, Nishiyama S, Harada N, Kakiuchi T. Evaluation of D-isomers of O-^{11}C-methyl tyrosine and O-^{18}F-fluoromethyl tyrosine as tumor-imaging agents in tumor-bearing mice: comparison with L- and D-^{11}C-methionine. *J Nucl Med.* 2006;47:679–88.
12. Urakami T, Sakai K, Asai T, Fukumoto D, Tsukada H, Oku N. Evaluation of O-[^{18}F]fluoromethyl-D-tyrosine as a radiotracer for tumor imaging with positron emission tomography. *Nucl Med Biol.* 2009;36:295–303.
13. Zitzmann-Kolbe S, Strube A, Frisk AL, et al. D-^{18}F-fluoromethyl tyrosine imaging of bone metastases in a mouse model. *J Nucl Med.* 2010;51:1632–1636.
14. Murayama C, Harada N, Kakiuchi T, et al. Evaluation of D-^{18}F-FMT, ^{18}F-FDG, L-^{11}C-MET, and ^{18}F-FLT for monitoring the response of tumors to radiotherapy in mice. *J Nucl Med.* 2009;50:290–295.
15. Suzuki H, Hasegawa Y, Terada A, et al. Limitations of FDG-PET and FDG-PET with computed tomography for detecting synchronous cancer in pharyngeal cancer. *Arch Otolaryngol Head Neck Surg.* 2008;134:1191–1195.
16. von Schulthess GK, Steinert HC, Hany TF. Integrated PET/CT: current applications and future directions. *Radiology.* 2006;238:405–422.
17. Kaira K, Oriuchi N, Shimizu K, et al. ^{18}F-FMT uptake seen within primary cancer on PET helps predict outcome of non-small cell lung cancer. *J Nucl Med.* 2009;50:1770–1776.
18. Kaira K, Oriuchi N, Otani Y, et al. Diagnostic usefulness of fluorine-18-alpha-methyltyrosine positron emission tomography in combination with ^{18}F-fluorodeoxyglucose in sarcoidosis patients. *Chest.* 2007;131:1019–1027.
19. Kaira K, Oriuchi N, Otani Y, et al. Fluorine-18-alpha-methyltyrosine positron emission tomography for diagnosis and staging of lung cancer: a clinicopathologic study. *Clin Cancer Res.* 2007;13:6369–6378.